Analysis of development process of landslide accumulation body based on discrete element method

Menglong Dong[1], Yukun Li[1], Yujiao Li[2]

[1]School of Earth Science and Engineering, Hohai University, Nanjing 210098, China
[2]Hebei electric power design and Research Institute, Shijiazhang 050000, China

Abstract. Large scale landslide accumulations are often seen in the construction of hydropower stations in Southwest of China. It is of great engineering significance to study the development process of these landslide accumulations and their development stages. In this paper, a landslide accumulation of a hydropower station is taken as the object of study. Through the three-dimensional discrete element analysis software 3DEC, the development process of the accumulation body is divided into five stages, and the deformation and failure characteristics of each stage are analyzed in detail. The research of this paper is of great help to guide the safety operation of the project.

1. Introduction

In recent years, with the construction of large hydropower stations in the southwest of China, giant landslides have great influence and restriction on the siting of new hydropower stations. The accumulation body is the product of the continued movement of the slope after deformation and failure [1]. Accumulation bodies, especially the accumulation bodies on the banks of the deep valleys of large rivers, are characterized by multiple stages and multiple functions. Because of different regional environment, geological conditions and geological tectonic movements, the accumulation bodies show different genetic mechanisms. In deep valleys, falling and landslides are the most common genetic types of accumulation. Under the incised and lateral erosion of the river, it is easy to form an open surface at the front edge of the high and steep bank slope. The bonding force between rock joints is weakened, and the outer surface of the steep slope is developed. The division of the layer makes the slope have the condition of falling [2]. The aging effect of the surface layer in the later stage, a large number of landslide accumulation bodies are often formed in the deep valley area.

Stability analysis of accumulation body is an important content in the study of accumulation. The commonly used methods are rigid body limit equilibrium and numerical simulation method. In recent years, numerical simulation has been widely used in rock slope calculation. The discrete element method, as an explicit numerical method, was proposed by Professor Cundall in 1971. Based on the discrete element method, ITASCA developed a commercial program 3DEC [3] [4] [5] [6]. It can simulate the mechanical response of a discontinuous medium (such as loose accumulation or jointed rock mass) subjected to static or dynamic loads.

In this paper, the three-dimensional discrete element method is used to simulate the loose structure of landslide accumulation. A landslide accumulation of a hydropower station in Southwest China is chose as subject, and the formation process and stability analysis of the accumulation are studied.

2. Overview of the project

A hydropower station is the fifth stage hydropower station of the planning river segment from Gushui to Miaowei of Lancang River, and it is located in Yingpan town Lanping county of Yunnan province. A road pass through the left bank of dam, and the distance of highway mileage away from Yingpan town is about 15km. It adjoins Tuoba hydropower station in the upstream. The normal reservoir water level is 1619m, the corresponding capacity is $14.18\times10^8 m^3$, and the installed capacity is 1900MW. The dam is preliminarily designed for RCC gravity dam, the elevation of dam crest is 1624m, the maximum height of dam is 202m, and the length of crest is 457m. The 500kV switch station is located on the upstream side of the left bank. The slope angle of natural slope is 40°-60°. The leading edge of the slope is steeper and the upper part is gentle. Because of the deep cutting of the Lancang River, the landform is the high mountain gravity accumulation landform. The front elevation of the accumulation is about 1490 meters, the back edge elevation is about 1850m, and the thickness is 10m~30m, show as Fig. 1. The total square of the accumulation is about $216\times10^4 m^3$, and the shape of accumulation is shown in the Figure 1. If the accumulation body of the switch station is failed, it will cause a certain effect on the operation of the power station and bring economic losses and casualties. Therefore, the study of the stability of the landslide accumulation has great significance to the safe operation of the hydropower station. The cross section of the slope shows in Fig. 2

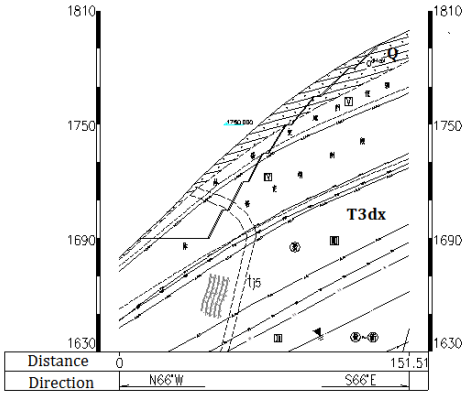

Fig. 1 Panorama of landslide accumulation **Fig. 2** Cross-section of landslide accumulation

Based on the geological information received from the project design company, the main lithological formations of the site are the Upper Triassic Xiaodingxi Formation (T3xd) and the Middle Jurassic Huakai Formation (J2h). The T3xd formation rocks consist of metamorphic tuff and volcanic conglomerate. The dip direction of the T3xd rock stratum is N10º-20ºE, and the dip angle is 75º-85º. The J2h formation rocks consist of phyllitic argillaceous slate and dark limestone. The surface of the natural slope is Quaternary slope colluvium (Q), which consists of crushed rock, clay and boulder, show as Fig. 3

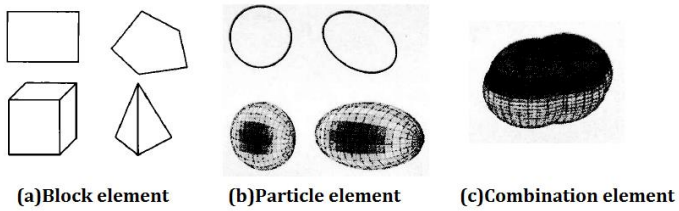

Fig. 3 Material of landslide accumulation **Fig. 4** Unit classification of discrete element

3. Introduction of discrete element method

3.1. Basic principle of discrete element method

In the discretization of objects, the discrete ideas of the discrete element method are similar to those of the finite element method. They all divide the areas under study into units and establish links between units through nodes. The element of discrete element method can be classified into two categories, block element and particle element, shown in Fig. 4. The most commonly used block elements are 4 body elements and 6 body elements. For two-dimensional problems, they can be arbitrary polygon elements, but their range of application is not wide. Each discrete element has only one basic node (take the centroid point). The particle element is mainly sphere element, and the disk element is used for the two-dimensional problem. The discrete element is a rigid body, and the relative deformation of the element is usually realized by the deformation element between the nodes. The deformation elements mainly include spring, kettle (damping), friction components and other physical forms of different forms of connection. Different combinations of basic components of various properties correspond to different constitutive relations. The mechanical form of connection can be divided into two categories, contact type and connection type [6] [7] [8].

3.2. Fundamental equations

In the discrete element method, the constitutive relationship between the force and the displacement of the equation of motion is the Newton's second law of motion. If the connection model is used, the displacement should be taken into account in accordance with the deformation coordination relationship. The kernel of the discrete element method is the second law of motion of Newton, that is, every element should be satisfied at any time, seen in Fig. 5. The equations of motion are as follows.

$$m_i \frac{d\upsilon_i}{dt} = \sum_{j=\xi_i(1)}^{\xi_{in}(ncontacti)} f_{ji}^{c} + f_i^{e} + b_i \tag{1}$$

$$I_i \frac{d\omega_i}{dt} = \sum_{j=\xi_i(1)}^{\xi_{in}(ncontacti)} f_{ji}^{cs} r_{ij} + M_i^{\theta} + M_i^{e} \tag{2}$$

Eq 1 is the equation of motion under the action of force.

Where, m_i is the quality of unit *i*. v_i is the centroid velocity vector of unit *i*. m_{ji}^{c} is the contact force of a unit *j*, which contact with unit *i*, effecting on unit *i*. It can be decomposed into the sum of normal force m_{ji}^{cn} and shear force m_{ji}^{cs} of contact line (surface) between unit *i* and unit *j*. m_i^{e} is external force of unit *i*. When the action of solid particles under the action of the flow field is studied, the nodal force acting on behalf of the fluid pressure is considered. b_i is bulk force of unit *i*. Eq 2 is equation of motion under the action of moment. I_i is moment of inertia of unit *i*. ω_i is angular velocity of unit *i*. r_{ij} is the distance from the effect point to the centroid unit *i*. M_i^{θ} is the moment of force produced by rotating spring. M_i^{e} is the moment external force. $\xi_{in}(ncontacti)$ is the series number of the unit j interacting with the unit *i*.

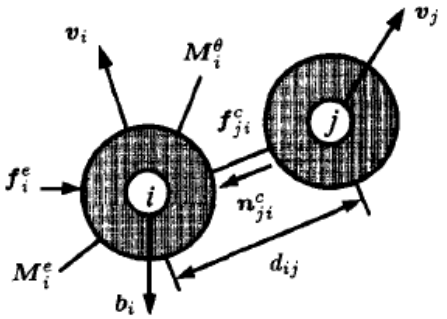

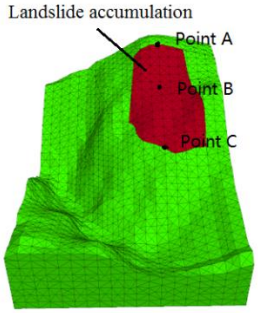

Fig. 5 Force and moment of element of discrete element **Fig. 6** Model of the slope

The solution of normal force and shear force can be solved by the relative displacement between two elements.

$$\begin{cases} f_{ji}^{cn} = -k_n \Delta u_{ji}^n + \eta_n \upsilon_{ji}^n \\ f_{ji}^{cs} = -k_s \Delta u_{ji}^s + \eta_s \upsilon_{ji}^s \\ M_i^\theta = -k_\theta \Delta \theta_i + \eta_\theta \omega_i \end{cases} \tag{3}$$

Where, k_n, k_s and k_θ are normal, shear and rotational spring elastic coefficients. η_n, η_s and η_θ are normal, shear and rotational spring damping coefficients. Δu_{ji}^n, Δu_{ji}^s and $\Delta \theta_i$ are three kinds of spring deformation.

The discrete element method is the constitutive relationship through relative displacement and force reflect specific materials, specifically by type and set the mode of spring element connected between models. Therefore, the selection of spring coefficients and damping coefficients is an important aspect of the discrete element method.

The relative velocity of the unit indirect contact may be derived from the following equation.

$$\upsilon_{ji} = \upsilon_{ji}^n + \upsilon_{ji}^s = (\upsilon_j - \upsilon_i) + d_{ij} n_{ji} \times (\omega_i + \omega_j) \tag{4}$$

Where, d_{ij} is the distance between the units, n_{ij} is the unit normal vector, and the direction is from j to i. The normal and shear relative displacement rates are obtained from follow equation.

$$\upsilon_{ji}^n = (\upsilon_{ji} \cdot n_{ji}) n_{ji}, \ \upsilon_{ji}^s = \upsilon_{ji} - (\upsilon_{ji} \cdot n_{ji}) n_{ji} \tag{5}$$

From Eq (4) and Eq(5), the element can be assumed to be rigid motion. The normal and shear relative displacements between units reflect the deformation of the material (continuum) and interaction between units (non-continuum). This reflects the geometrical relation of the material under the condition of deformation. The of motion equations (Eq 1 and Eq 2), constitutive equations (Eq 3), and geometric equations (Eq 4 and Eq 5) form the basic equations of discrete elements. The plasticity and failure of materials can be simulated by connection element. The local failure of the material can be simulated by the fracture of the spring between the elements. The plastic behavior of the material can be simulated by restricting the deformation of the spring and changing the stiffness of the spring.

4. Modelling

4.1. Geological modelling

The establishment of the slope model was mainly based on field investigation of the hydropower station, including bedrock morphology, topography, geomorphology, stratigraphic lithology and structural features, etc. The original slope could be inferred from the existing topographic map. According to the estimated volume of the accumulated body on the spot, it was restored to the original geomorphic and the corresponding rock mass structure characteristics. Three dimensional dynamic numerical simulations were used to reproduce the deformation, failure and accumulation process. The model was modeled by Sufer software, and the slope coordinate points were discretized properly. The point information was imported into the 3D discrete element software 3DEC, and then the dynamic simulation of the deformation and failure accumulation process were carried out in 3DEC. Shown as Fig. 6

4.2. Setup of the Numerical Model

In the model, X axis was south direction, Y axis was east direction, and Z axis was vertical direction. Considering the computational capability of the software, the model was simplified to some extent on the basis of the actual topography and the structure of rock mass. But the simplified model did not affect the analysis of the actual situation. The elastic plastic Mohr-Coulomb model was used for the mechanical behavior of T3dx, J2h and Q rock masses in the model. The rock mass mechanical properties used in the 3DEC numerical modeling are listed in Table 1. The Coulomb slip model was used for all the faults and contacts in the 3DEC model. The discontinuity mechanical properties used in the modeling are listed in Tables 2.

Table 1. Estimated rock mass mechanical parameter values

Rock type	J2h (Slate)	T3xd (Tuff)	Q (Quaternary)
Cohesion, c (MPa)	0.85	1.5	0.1
Friction angle, φ (°)	32	42	22
Density (Kg/m³)	2530	2612	2245
Poisson's ratio	0.33	0.24	0.38
Modulus of deformation, E_r (GPa)	10	18.5	0.8
Bulk modulus, K_r (GPa)	1.13	3.2	0.01
shear modulus, G_r (GPa)	6.65	11.47	0.55
Tensile strength (MPa)	2.8	3.4	0

Table 2. Estimated geo-mechanical parameter values of the discontinuities

Discontinuity type	Cohesion (MPa)	Φ (°)	Normal stiffness JKN (Pa/m)	Shear stiffness JKS (Pa/m)
Faults	0.024	16	4×10^9	9.5×10^8
Contacts (of the two strata)	0.051	22	6.6×10^9	1.25×10^9
IV and V structural planes	0.048	20	5×10^9	1.1×10^9

The vertical in-situ stress was increased from the top of the model to the bottom of the model according to the gravitational loading. The horizontal in-situ stress was increased from the top of the model to the bottom of the model according to the gravitational loading and the lateral stress ratios in the horizontal direction. In this model, the vertical stress is obtained by gravity, and the horizontal stress is half of the vertical stress.

5. Analysis of results

According to the discrete element software 3DEC, the original slope model was simulated. As shown in Figure 6, the displacements of A, B, and C three points were monitored at the back edge, the middle edge, and the front edge. After the 1000 steps of the iteration, the whole slope failed. The displacements of the three monitoring points along the Z and Y directions were shown in Fig. 7 (a) and (b), respectively.

It can be seen from Fig. 7(a), the displacements of B and C points in the Z direction (vertical direction) were mainly divided into five stages. ①Before 100 steps, there were no large displacement change in monitoring points. ②Between 100 and 250 steps, the rate of displacement curve was obviously larger, which indicated that the displacement of two points was obvious, and the slope was rapidly deformed in vertical direction. ③Between 250 and 600 steps, the displacement velocity of two points were obviously slower, and the failure of slope was not obvious. ④After 600 steps, the displacement of the two points changed rapidly. ⑤The slope was completely destroyed. However, the vertical displacement of the A point changed at a higher speed during the whole deformation and failure process. It was shown that the back part of the potential sliding body was the first to destroy, and it was sensitive to the deformation of the slope.

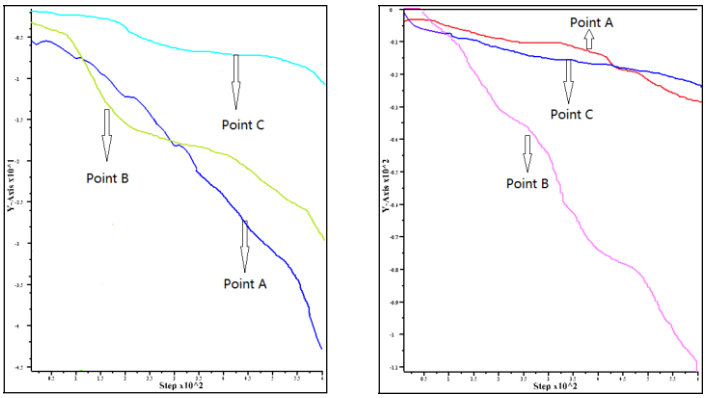

(a) (b)

Fig. 7 Displacements of three monitoring points: (a) Z-direction and (b) Y-direction (cm)

The displacement of B point in Y direction was divided into 5 stages, shown in Fig. 7(b). ①Before the 80 steps, the displacement in the Y direction was almost unchanged. ②Between 80 and 200 steps, B point had obvious displacement and rapid deformation in Y direction. ③Between 200 and 600 steps, the displacement rate of the B point in the Y direction was obviously slowed down. ④After 600 steps, the displacement of the B point was obviously shifted again. ⑤The slope was completely destroyed. The displacements of A and C points in the Y direction had a steady state from the beginning of the slope deformation to failure. It was shown that the displacements of A and C points were not sensitive to the displacements in the Y direction during the whole deformation and failure process.

According to the above dynamic simulation results, the formation process of the original slope accumulation on the left bank can be divided into five stages: local displacement stage, first transition stage, strong tensile fracture stage, second transition stage and whole sliding stage. The five stages of deformation and failure process were analyzed and explained respectively based on the deformation of slope, shear stress of A cross section (cross section of monitoring point A and parallel to YZ plane) and velocity vector diagram of discrete units at different stages of computation.

(1) Local displacement stage

In this stage the original valley was eroded and cut down, the original stress balance of the slope was broken, the lateral stress was weakened, and the unloading phenomenon was produced. There were tensile cracks and displacement occurs at the local slope. The rock mass had only a slight change

of angle, and there was no obvious shear displacement or rolling failed. The slope was still in a stable state.

It can be seen from Fig. 8 and 9, there is no obvious deformation and displacement in the front edge of the potential landslide. Only tiny displacement occur only in the middle and back part of the potential landslide.

(2) First transitional stage

After the slope passes through the local displacement stage, balanced state of the inner stress in the slope was broken because of the local deformation. However, due to the self-stability of the slope, the stress recombination occurs automatically in the slope, and the reconstructed slope can remain stable. It can be seen from Fig. 10 and 11, the shear stress in the slope has changed, the maximum shear stress range is slightly larger than the previous stage, and appears farther away from the slope surface. Because the deformation of the local displacement stage is small and the process duration is short, the initial stress reconstruction is relatively easy and the process is relatively short.

(3) Strong tensile fracture stage

After the initial stress reorganization of the left bank slope, the slope reaches the stress balance again. But with the river valleys keeping cut, the stress balance on the left bank slope will be broken again. With the local displacement occurring at the two previous stages, a slight tension crack has been appeared inside the slope. With the constant cutting of the river valley, the unloading effect becomes more and more obvious, and the small tensile fracture in the slope is developed, which makes the slope deform larger.

It can be seen from the Fig. 12 and 13, at this stage, the slope has occurred obvious deformation, the back edge of the sliding surface has obviously fallen, and the displacement of each element of the sliding body is obvious. The protruding tongue of landslide is obvious.

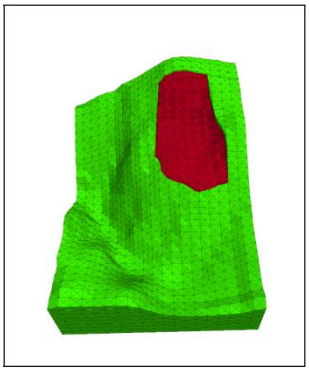

Fig. 8 Slope deformation diagram in 200 steps

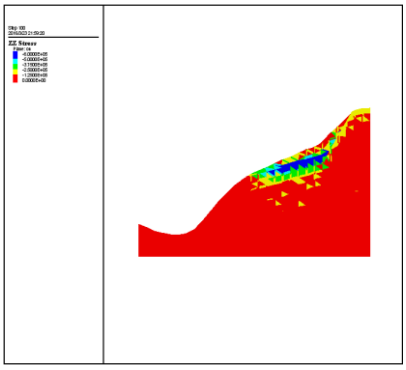

Fig. 9 Shear stress distribution of A section in YY direction in 200 steps

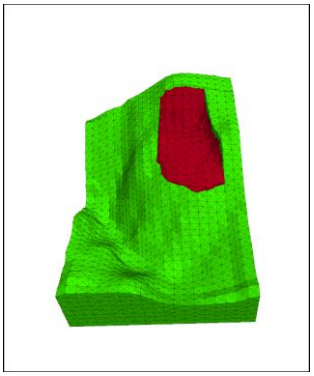

Fig. 10 Slope deformation diagram in 400 steps

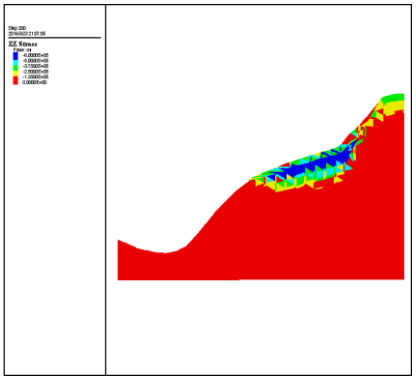

Fig. 11 Shear stress distribution of A section in YY direction in 400 steps

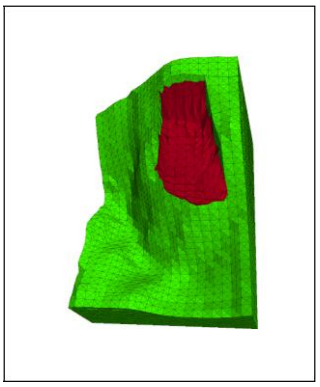

Fig. 12 Slope deformation diagram in 600 steps

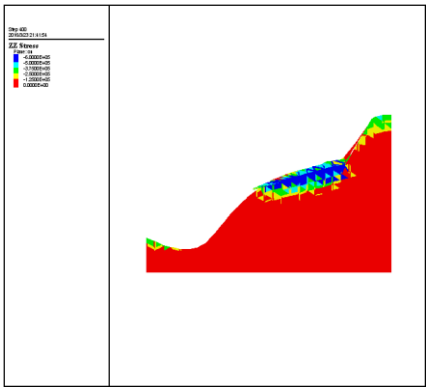

Fig. 13 Shear stress distribution of A section in YY direction in 600 steps

(4) Second transitional stage

After the rapid decline in the last stage, the stress in the interior of the slope becomes balanced again, and the development trend of deformation and failure becomes slow. The deformation of the front and back edges of the sliding surface develops slowly shown in Fig 14. The displacement of each discrete element of the potential sliding body is smaller, and the displacement of each element of the front edge of the sliding surface is smaller than that of the front shown in Fig 15. From the view of the cross section, there is no obvious development of the back edge of the landslide tongue and the sliding surface. But the shear stress changes.

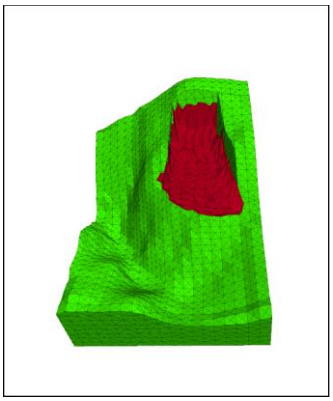

Fig. 14 Slope deformation diagram in 800 steps

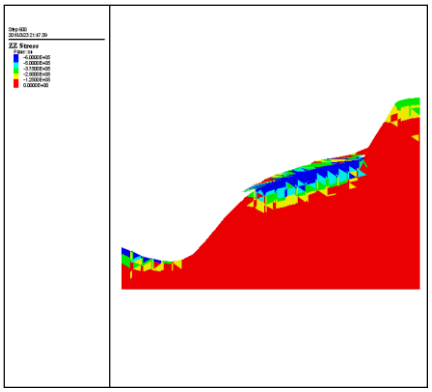

Fig. 15 Shear stress distribution of A section in YY direction in 800 steps

(5) Whole sliding stage

After second transition stages, the stress state in the slope is changed. After the four stages of development, the cracks in the slope of the structural plane linked up, forming a control structure surface, thus making the slope instability and failed. It can be seen from Fig. 16, the front edge of the sliding surface has fanned out, and the discrete unit at the back edge has also appeared severe deformation under the action of tensile stress. In Fig. 17, the back edge of the landslide has a complete destruction and separate from the behind wall. Potential sliding body has undergone whole destruction.

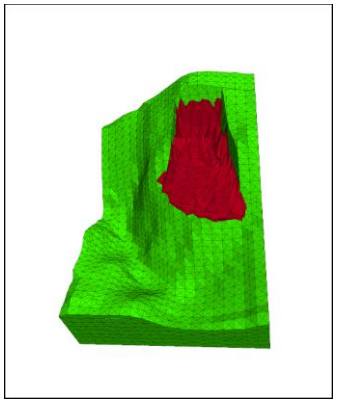

Fig. 16 Slope deformation diagram in 1000 steps

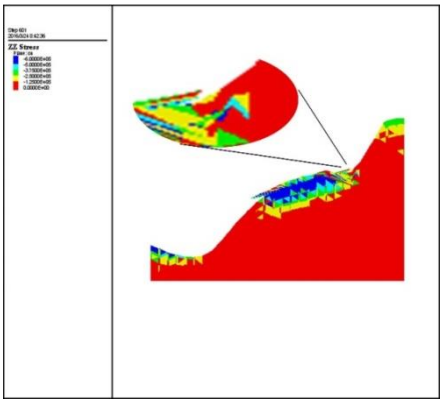

Fig. 17 Shear stress distribution of A section in YY direction in 1000 steps

6. Conclusion

By taking a landslide accumulation body of a power station as the object of study, the formation process of the accumulation body is studied. The formation of this accumulation process is divided into 5 stages: local displacement stage, first transition stage, strong tensile fracture stage, second transition stage and whole sliding stage.

In the process of stream trenching and headward erosion, the stress balance of the slope is broken because of the unloading. Unloading rebound occurs in rock mass, resulting in tension cracks in the back edge. With the cutting of the river valley, the unloading continues to increase, and the micro cracks in the slope continue to expand. Originally discontinuous and cracks have been linked together in their own development, resulting in higher grade structural planes, and then developing into controlled structural planes. The controlled structural planes form a potential sliding surface for the slope. During the history of stream trenching, potential sliding body experienced the five stages of development, and finally produced complete deformation and failure. Finally, the landslide slides and deposits again at low elevation, which makes the slope form a new geomorphic morphology: the upper part is steep, the middle is gentle, and the lower part is steep. The causes of most landslide accumulation bodies in the high mountain gorge region of Southwest China can be summarized as the above 5 stages.

References

[1] Zhang ZY. Principles of engineering geology analysis, Beijing. 1994.
[2] Morgenstern, N.R.,and Price surfaces. Geotechnique, London, V.E. The analysis of the stability of general slip,1965; 15 (1), 79-93.
[3] Cundall PA. Formulation of a three-dimensional distinct element model-Part 1. A scheme to detect and represent contacts in a system composed of many polyhedral blocks. Int J Rock Mech Min Sci & Geomech Abstr. 1988; 25, 107-116.
[4] Itasca. 3DEC 3-Dimensional Distinct Element Code User's Guide. Itasca Consulting Group Inc. 2007.
[5] Cundall P.A., Hart RD, 1992. Numerical modelling of discontinua. Eng Comput. 9,101–113.
[6] Firpo G., Salvini R., Francioni M., Ranjith G.P., 2011. Use of digital terrestrial photogrammetry in rocky slope stability analysis by distinct elements numerical methods. Int J of Rock Mech & Min Sci. 48, 1045-1054.
[7] Hart R., Cundall P.A., Lemos, J., 1988. Formulation of three-dimensional distinct element model, Part Ⅱ, Mechanical calculation of a system composed of many polyhedral blocks. Int J Rock Mech Min Sci Geomech Abstr. 25(3), 117-125.
[8] Lei Y., Wang S., 2006. Stability analysis of jointed rock slope by strength reduction method based on UDEC. Rock and Soil Mechanics, China, 27(10):1695-1698.